Tropical Plant Pathology (2024) 49:367–383
https://doi.org/10.1007/s40858-024-00636-6

ORIGINAL ARTICLE

Prevalence of mango stem-end rot disease in Côte d'Ivoire and identification of associated fungal pathogens

Yefoungnigui Souleymane Yeo[1,2,3] · Yassogui Kone[1,2] · Dio Dramane Dembele[2,4] · Elisee Ler-N'Ogn Dadee Georges Amari[1,2] · Jean-Yves Rey[5] · Emerson Medeiros Del Ponte[6] · Diana Fernandez[3] · Daouda Kone[1,2]

Received: 30 August 2023 / Accepted: 3 January 2024 / Published online: 26 February 2024
© The Author(s), under exclusive license to Sociedade Brasileira de Fitopatologia 2024

Abstract

The Stem-end rot (SER) postharvest disease of mango (*Mangifera indica* L.) fruits is a significant economic threat to mango production. Without proper management strategies, it can lead to up to 100 % postharvest losses. Despite its importance, very little information is known about this disease in Côte d'Ivoire. This research aimed to determine the incidence and severity of SER in mango orchards, assess how preharvest climate parameters affect the disease and determine the pathogenic fungi associated with SER. Mango SER was evaluated on 1500 mango fruits collected from 15 orchards in Boundiali, Ferkéssédougou, Korhogo, Odienné, and Sinématiali departments. Mango SER incidence ranged from 10 % to 30 %, while severity ranged from 5 % to 20 %. No significant differences in these parameters were observed between the different departments ($P>0.05$). The study also revealed a positive low correlation between SER disease incidence and mean air temperature ($r = 0.36$) and minimum air temperature ($r = 0.26$) data, indicating that preharvest weather conditions may have a marginal impact on mango SER disease intensity in the postharvest phase. Pathogenic fungi associated with SER were isolated and identified using morphological characteristics and multilocus sequence analysis of the rDNA internal transcribed spacer (ITS) region and the translation elongation factor 1-alpha (*tef1-α*). Various fungal species associated with mango SER disease were also identified, with *Lasiodiplodia* species (74%) being the most prevalent (including *Lasiodiplodia theobromae, L. euphorbicola*, and *L. caatinguensis*), followed by *Colletotrichum gloeosporioides*, *Curvularia pseudobrachyspora*, *Diaporthe endophytica* and *Fusarium mangiferae*. However, only *Lasiodiplodia* species and *Diaporthe endophytica* induced SER symptoms. This study was the first ever evaluation of mango SER disease and associated fungal pathogens identification in Côte d'Ivoire. This result will assist researchers in developing a control method for mango SER.

Keywords Botryosphaeraceae · Climate · Epidemiology · Postharvest disease · Pathogenic fungi

Diana Fernandez and Daouda Kone are co-last author.

✉ Diana Fernandez
diana.fernandez@ird.fr

[1] UPR Physiologie et Pathologie Végétale, Université Félix HOUPHOUËT-BOIGNY, UFR Biosciences, 22 BP 582, Abidjan 22, Côte d'Ivoire

[2] WASCAL / African Center of Excellence in Climate Change, Biodiversity and Sustainable Agriculture, Pôle Scientifique et d'Innovation, Bingerville, Université Félix HOUPHOUËT-BOIGNY (UFHB), 01 BP V 34, Abidjan 01, Côte d'Ivoire

[3] UMR PHIM (Plant Health Institute), Univ. Montpellier, IRD, CIRAD, INRAE, Institute Agro, Montpellier, France

[4] UFR Sciences Biologiques, Département de Biologie Végétale, Université Péléforo GON COULIBALY (UPCG), B. P 1328, Korhogo, Côte d'Ivoire

[5] HortSys, Université Montpellier, CIRAD, Montpellier, France

[6] Departamento de Fitopatologia, Universidade Federal de Viçosa, Viçosa, MG 36570-900, Brazil

Introduction

Mango (*Mangifera indica* L.) is a highly valued fruit produced in tropical, subtropical, and semi-arid regions. According to FAOSTAT (2021), the global production of mangoes is estimated at over 57 million tons. Mangoes are rich in fibre and nutrients such as, vitamins C and A, polyphenols, carotenoids, carbohydrates, and calcium (Owino and Ambuko 2021). However, mango production is threatened by several fungal diseases, including postharvest Stem-end rot (SER). The SER disease is characterized by small dark-brown lesions in the peel surrounding the fruit stem end, eventually leading to soft and watery decay, causing complete fruit rot (Galsurker et al. 2020). Without proper management strategies, the disease can significantly reduce fruit quality and may result in postharvest losses of up to 100% in some orchards (Honger and William 2015; Alam et al. 2017).

Several fungal species have been associated with mango SER, including *Neofusicoccum brasiliense*, *N. parvum*, *N. mangiferae*, *Fusicoccum aesculi*, *Nattrassia mangiferae*, *Neoscytalidium dimidiatum*, *Lasiodiplodia theobromae*, *Curvularia* sp, *Fusarium* sp, *Neocosmospora* sp, *Pestalotiopsis* sp, *Neopestalotiopsis* sp, *Colletotrichum gloeosporioides*, and *Alternaria* sp. (Johnson et al. 1992; Marques et al. 2013; Phillips et al. 2013; Alam et al. 2017; Adikaram et al. 2022). The psathogen may colonize inflorescence and pedicel tissues during flowering and remain as endophyte in phloem and xylem vessels (Johnson et al. 1992). Infected fruits may remain asymptomatic until ripening, making detection difficult for farmers during harvest (Govender et al. 2005). As a result, the disease is often identified during storage and transportation, which is a challenge for effective control (Johnson 2008; Terao et al. 2018).

Mango production contributes significantly to the economy of Côte d'Ivoire, generating over 10 million euros of income for local communities, corresponding to 4 % of the country's gross domestic product (GDP) (Pugnet 2018). The country is the third largest supplier of mangoes to the European Union market, after Brazil and Peru (Pugnets 2018). However, despite significant initiatives by the government and private sector, mango production in Côte d'Ivoire still faces a substantial challenge in the form of postharvest losses. These losses account for approximately 30 to 35% of the country's total mango production, resulting in an economic impact of around 5 million euros (Kouassi 2012). Reducing these losses through control strategies can significantly enhance the mango sector contribution to the country's economy and improve the livelihoods of local communities. Prior research in Côte d'Ivoire on mango postharvest fungal diseases has mainly focused on anthracnose diseases caused by *Colletotrichum* species (Kouamé et al. 2011; N'Guettia et al.2014; Dembélé et al. 2020). While anthracnose may be well controlled with fungicide application, mango SER still has a significant economic impact for producing countries (Galsurker et al. 2018; Karunanayake and Adikaram, 2020).

Several factors, including climatic parameters such as temperature and relative humidity have been reported that affect mango SER (Diedhiou et al. 2007; Alkan and Kumar 2018), probably by impacting directly pathogen infection (Riquelme-Toledo et al. 2020). Therefore, weather parameters may impact the inflorescence colonization rate by endophytic fungi during flowering, which could influence the incidence and severity of SER. Understanding the potential impact of weather parameters on SER disease is essential for developing effective control strategies. The objective of this research is three-fold: firstly, to assess the incidence and severity of mango SER in Côte d'Ivoire; secondly, to examine the relationships between preharvest climate conditions and the incidence and severity of SER; and thirdly, to identify the specific fungal agents causing SER.

Material and methods

Orchards surveys and SER evaluation

Mango SER was evaluated on mango fruits (cv. Kent) at physiological maturity, collected from 15 mango orchards located in the departments of Korhogo, Sinématiali, Ferkéssédougou, Boundiali, and Odienné. These regions are the main mango production areas in the country. Three orchards located at least 5 km apart with a similar age (>30 years) were selected in each department. Then 100 fruits were harvested from 20 randomly selected trees in each orchard.

Fruits external surface was disinfected using a 5% hypochlorite solution, then rinsed with tap water and air dried for 30 minutes. Fruits were then packed by orchards and stored in a cold room with a temperature of 14.5 ± 0.5°C and relative humidity of 80 ± 2 % for two weeks to simulate sea-shipment transportation from Côte d'Ivoire to the European market. Then, fruits were transferred to another room with temperatures ranging from 31 ± 5°C and relative humidity of 70 ± 5% to accelerate the fruits' ripening. SER symptoms were observed weekly for 28 days (incubation period). The severity index of each fruit was determined using a severity scale adapted from Alvindia and Acda (2015) ranking from 0 to 6, where 0 = no discoloration of the stem-end, 1 = discoloration limited at the stem-end, 2 = 10% discoloration of the fruit surface area initiated by stem-end rot, 3 = 11-30% discoloration of the fruit surface area initiated by stem-end rot, 4 = 31-50% discoloration of the fruit surface area initiated by stem-end rot, 5 = more

Table 1 Incidence and severity of SER in fifteen localities from five departments in Côte d'Ivoire. Different letters in column indicate a significant variance ($P<0.05$) analysed by Tukey's range test

Department	SER incidence (%)	SER severity (%)	Locality	SER incidence (%)	SER severity (%)
Sinematiali	12 ± 2.0^{a}	9.4 ± 2.8^{a}	Klolikaha	12 ± 0.60^{a}	7.6 ± 0.26^{a}
			Donassokaha 1	14 ± 3.32^{a}	11.2 ± 0.46^{a}
			Donassokaha 2	10 ± 0.19^{a}	5.6 ± 2.60^{a}
Korhogo	14.7 ± 3.0^{a}	11.8 ± 1.3^{a}	Tioroniaradougou	12 ± 1.43^{a}	9.6 ± 0.26^{a}
			Sissian	18 ± 1.60^{a}	11.6 ± 0.60^{a}
			Oualokaha	14 ± 3.02^{a}	12 ± 0.46^{a}
Boundiali	11.3 ± 5.0^{a}	7.6 ± 2.8^{a}	Boundiali 1	12 ± 0.46^{a}	7.2 ± 0.12^{a}
			Boundiali 2	16 ± 0.40^{a}	8 ± 0.60^{a}
			Boundiali 3	6 ± 0.41^{a}	2.8 ± 0.70^{a}
Odienne	19.3 ± 13.0^{a}	19.8 ± 10.0^{a}	Odienné 1	6 ± 0.70^{a}	4 ± 2.60^{a}
			Odienné 2	32 ± 1.60^{b}	24 ± 1.46^{b}
			Odienné 3	20 ± 2.30^{b}	15.6 ± 0.46^{a}
Ferkessedougou	22 ± 7.2^{a}	17.4 ± 3.9^{a}	Village A	16 ± 0.60^{a}	10.8 ± 0.29^{a}
			Tchékpè	20 ± 9.06^{b}	18.4 ± 0.60^{b}
			Ferkéssédougou	30 ± 9.07^{b}	16.4 ± 2.60^{a}

than 51% discoloration of the fruit surface area initiated by stem-end rot, 6 = 100 % discoloration of fruit surface. The incidence (DI) and severity (DS) of postharvest SER disease were calculated for each orchard using the following formulas:

$$\mathrm{DI}\ (\%) \frac{(\text{Number of fruit showing SER sypmtoms})}{\textit{Total number of fruit}} \text{x} 100$$

$$\mathrm{DS}\ (\%) = \frac{\sum(\text{Severity i of the disease of the fruit X Number of the fruit of severity i})}{\text{Total number of fruit harvested X Highest number on the severity scale}} \text{x}\ 100$$

Climate data source

In order to evaluate the correlation between climate parameters and SER incidence and severity, we downloaded monthly climatic data such as Relative Humidity at 2 meters above ground (RH2M), Dew point temperature at 2 meters above ground (T2MDEW), maximum air temperature at 2 meters above ground (T2M_MAX), average air temperature at 2 meters above ground (T2M) and the minimum air temperature at 2 meters above ground (T2M_MIN), spanning six months prior to the survey (November to April 2021) from the National Aeronautics and Space Administration (NASA) POWER project *via* the nasapower R package version 4.0.9 (Sparks, 2018). Data were downloaded using the geographic coordinates (latitude and longitude) of the 15 orchards surveyed across the departments surveyed. The six months average data of each climatic variable were then correlated with SER postharvest incidence and severity.

Fungal isolation

The fruits showing SER symptoms were washed briefly using distilled water. Five fragments measuring 5x5 mm^2 were cut from the margin between symptomatic and asymptomatic tissues. Fragments were surface sterilized by dipping them in 70 % ethanol for one minute, then in a 5 % sodium hypochlorite (NaClO) solution, and then rinsed three times with distilled sterile water. After sterilization, fragments were briefly dried on sterile filter paper. Five fragments were placed on each Petri dish (9 cm diameter) containing potato dextrose agar medium (PDA) and incubated at room temperature at 25 °C in darkness for one week. Cultures were checked daily for hyphal growth, and emerging hyphae were transferred to a new PDA plate. Fungi that did not sporulate on PDA were cultured on a 2 % water-agar (WA) containing sterilized pine (*Pinus nigra* Arnold) needles and incubated at 25 °C with a 8 h photoperiod for four weeks to induce the formation of fruiting bodies and sporulation. Fresh culture of single spore fungal pure cultures of each isolate was conserved (on toothpicks sticks at 5°C) at Félix Houphouët-Boigny University in Côte d'Ivoire.

Morphological identification of SER fungal isolates

The macro-morphological characteristics of fungal colonies, such as mycelium appearance, colour and spore production, were assessed from single spore-conidial cultures

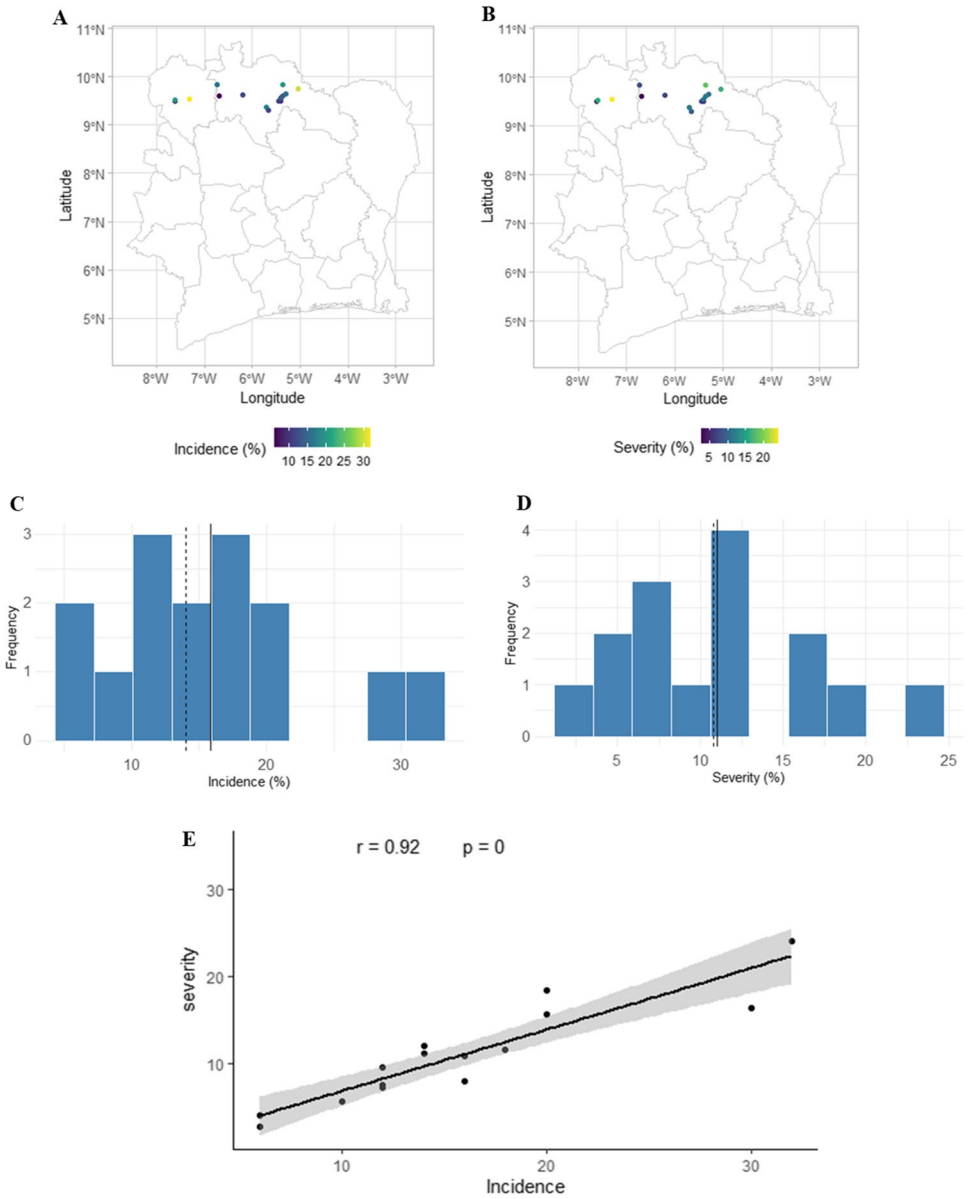

Fig. 1 Distribution map and frequency of mango SER incidence (**A**, **C**) and severity (**B**, **D**) of mango SER postharvest disease in 15 orchards from Côte d'Ivoire and the correlation between both variables (**E**)

grown on PDA or WA. Conidia and conidiogenous cells were observed from material mounted in lactic acid under a light microscope (Zeiss Z2, Alen, Germany), and some characteristics of conidia (shape, size, colour, longitudinal striations and presence or absence of septum) were recorded. Photographs were made using an Axiocam 506 colour camera with Zeiss Image Z2 software. Morphological characters were used to identify the fungi isolated to the genus level.

DNA extraction, PCR amplification and sequencing

Based on morphological characters and pathogenicity test, the isolates Fr-F01; FRK37, FRZ20, FRZ27, SA9FSy, BenFFSy, and NTA were selected for molecular identification (Table 2). Fungal isolates were cultured on PDA and incubated at 25 °C for 5 days. About 20 mg of mycelium was scraped and ground with a disposable pestle mounted on an electric homogenizer (Dutscher, France) into a 1.5 ml tube containing 50 µl of freshly prepared 0.5 M sodium hydroxide (NaOH). The total genomic DNA was extracted using a rapid extraction protocol of Groppe and Boller (1997). The internal transcribed spacer (ITS) and elongation translation factor (*tef1-α*) genes sequences were amplified by Polymerase chain reaction (PCR) assays and sequenced using primer pairs, ITS4 (TCCTCCGCTTATTGATATGC) / ITS5 (TCCTCCGCTTATTGATATGC) (White et al. 1990) and EF1-688F(CGGTCACTTGATCTACAAGTGC) / EF1-1251R (CCTCGAACTCACCAGTACCG) (Alves et al. 2008), respectively. For each PCR reaction,

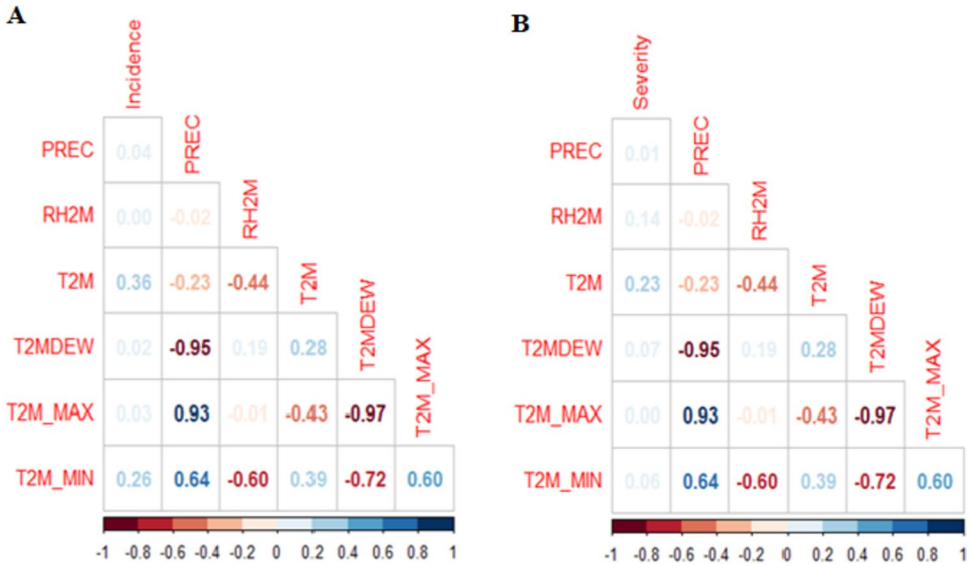

Fig. 2 Correlation matrix of mango SER and weather parameters: **A**= Incidence; **B**= Severity. PREC= precipitation; RH2M= Relative Humidity at 2 meters above ground; T2MDEW =Dew point temperature at 2 meters above ground; T2M_MAX= maximum air temperature at 2 meters above ground; T2M= average air temperature at 2 meters above ground; T2M_MIN = minimum air temperature at 2 meters above ground

a mixture (25 µl) was prepared, which contained 5 µl of 5x Green GoTaq buffer, 2 µl of deoxynucleotide triphosphate polymerase (dNTPs) (5 mM), 1 µl of each primers (10 µM), 0.125 µl of GoTaq G2 polymerase (Promega, France), 14.875 µl of sterile Milli-Q water, and 2 µl of genomic DNA. PCR was realized with a MyCycler™ Thermal Cycler following these different steps: initial denaturation at 94 °C for 2 min, then 30 cycles of denaturation at 94 °C for 30 s (ITS) and 95 °C for 30 s (*tef1-α*), annealing at 58°C for 30 s (ITS) / 55 °C for 45 s (*tef1-α*), elongation at 72°C for 30 s (ITS) / 90 s (tef1-α), and final elongation at 72°C for 8 min (ITS)/10 min (*tef1-α*). The PCR products were separated by electrophoresis for 20 min at 100 V in a 1 % agarose gel stained with ethidium bromide. The gel was viewed and photographed using the Bio-Rad Molecular Imager® Gel Doc™ XR System and Bio-Rad Quantity One® Software. The size of the amplified PCR products was ascertained by utilizing a 100 bp GeneRulers™ DNA ladder (Promega). PCR products were sent to Genewiz/ Azenta company for DNA sequencing in both directions.

Sequence alignment and phylogenetic analyses

Raw ITS and *tef1*-α sequences were trimmed, aligned, and manually adjusted, and consensus sequences were generated with the BioEdit version 7.2.5 software (Hall 1999). The genetic relatedness of the ITS and *tef1*-α of isolates sequences with other fungal sequences in the GenBank database was determined using the nucleotide Basic Local Alignment Search Tool (BLASTN) (https://blast.ncbi.nlm.nih.gov/Blast.cgi) with default parameters. All sequences obtained were deposited in the GenBank database (Table 2). Based on the best BLASTN homology results, different ITS and *tef1-α* datasets were used to assess the phylogenetic positions of SER isolates. We retrieved in GenBank the sequences from well characterized isolates (type collection) of *Lasiodiplodia*, *Colletotrichum*, *Curvularia*, *Fusarium* and *Diaporthe* species (Table 2). Prior to phylogenetic analysis, ambiguous sequences at the start and end were deleted in order to optimize the alignments. Multiple sequence alignments of SER isolates and reference type collection sequences were generated using the default settings of the ClustalW algorithm in MEGA 11 software (Tamura et al. 2021). Alignment parameters were applied to find the best nucleotide substitution model in MEGA 11 with the Bayesian Information Criteria (BIC) and Akaike Information Criteria (AIC). Phylogenetic analysis was conducted using the maximum likelihood (ML) method. The Nearest Neighbor Interchange (NNI) heuristic method was used for trees inference. The initial tree was automatically generated using the Maximum Parsimony method. The ML trees were generated with 1000 bootstrap replications. All analyses were performed using MEGA 11 software (Tamura et al. 2021).

Pathogenicity tests

Pathogenicity tests of SER isolates were realized on mature, asymptomatic, without any visible signs of blemishes mango fruits (cv Kent). Fruits were surface sterilized by deeping them in 1 % NaClO solution for 10 min and rinsed three times with sterile distilled water before being air dried for 30 min. Using a sterile scalpel, 1 cm^2 of surface tissue was excised from the fruit at the peduncle. A 5-mm fungal mycelial plug of 7-day-old culture of each isolate prepared on PDA was used to inoculate fruits,

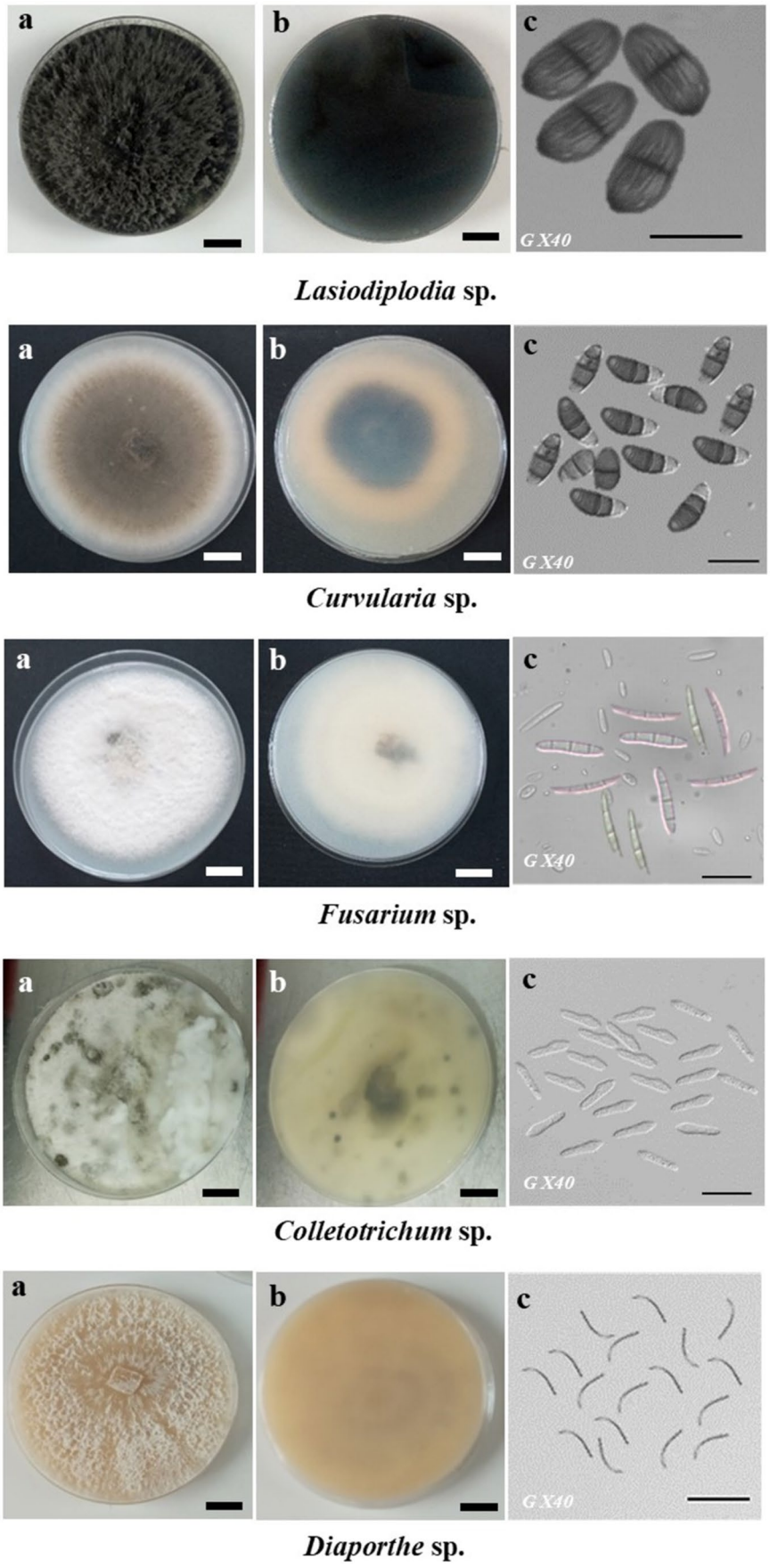

Fig. 3 Colony and conidia morphology of *Lasiodiplodia* sp., *Curvularia* sp., *Fusarium* sp., *Colletotrichum* sp., *Diaporthe* sp. grown on PDA: (**a**) upper, and (**b**) lower surface appearance, (**c**) conidia. Scale bars (**a**, **b**) = 2 cm; (**c**) = 20 µm

Table 2 Characteristics of the isolates selected for molecular identification of fungi associated with mango Stem-end rot

Isolate	Species*	Length of conidia (µm)	Width of conidia (µm)	Average L/W of conidia	GenBank Accession numbers	
					ITS	*tef1-α*
BenFFSy	*Curvularia pseudobrachyspora*	17.2-26	9-11	2.7	OR264470	OR287046
SA9FSy	*Colletotrichum gloeosporioides*	15-18.0	5-6	3	OR264469	OR338285
1BRaA2	*Fusarium mangiferae*	Macroconidia (22.5-37.1)	2-3.6	10.6	OR264471	OR287047
NTA	*Diaporthe endophytica*	Beta conidia (19-25)	1-1.6	16.9	OR264472	OR287048
Fr-F01	*Lasiodiplodia theobromae*	19.8-27.7	10.8-14.2	1.8	OQ067836	OQ269654
Fr-K37	*Lasiodiplodia euphorbicola*	16.5-31.6	11.9-15.22	1.9	OQ067837	OQ269655
Fr-Z20	*Lasiodiplodia euphorbicola*	20.7-26.4	10-14.3	1.9	OQ067838	OQ269656
Fr-Z27	*Lasiodiplodia caatinguensis*	15.4-25.5	12.1-15.1	1.7	OQ067839	OQ269657
CERC1961	*L. americana*	-	-	-	KP217059	KP217067
CMW41467	*L. avicenniae*	-	-	-	KP860835	KP860680
CMM4015	*L. brasiliense*	-	-	-	JX464063	JX464049
CMW41470	*L. bruguierae*	-	-	-	KP860833	KP860678
IBL366	*L. caatinguensis*	-	-	-	KT154760	KT008006
IRAN1522C	*L. citricola*	-	-	-	GU945354	GU945340
CMW33266	*L. crassispora*	-	-	-	KU887072	KU886951
BOT10	*L. egyptiacae*	-	-	-	JN814397	JN814424
CMM3609	*L. euphorbicola*	-	-	-	KF234543	KF226689
BL104	*L. exigua*	-	-	-	KJ638317	KJ638336
CMW14077	*L. gonubiensis*	-	-	-	AY639595	DQ103566
MSBN-2015	*L. gravistriata*	-	-	-	KT250949	KT266812
IRAN1500C	*L. hormozganensis*	-	-	-	GU945355	GU945343
IRAN921C	*L. iraniensis*	-	-	-	GU945346	GU945334
CMM3610	*L. jatrophicola*	-	-	-	KF234544	KF226690
CBS167.28	*L. laeliocattleyae*	-	-	-	MH866448	KU507454
CMW54165	*L. lignicola*	-	-	-	MT934413	MT920442
CMM3833	*L. macrospora*	-	-	-	KF234557	KF226718
MFLUCC18-0948	*L. magnoliae*	-	-	-	MK499387	MK568537
CMW27801	*L. mahajangana*	-	-	-	FJ900595	FJ900641
BL1	*L. mediterranea*	-	-	-	KJ638312	KJ638331
UCD2193MO	*L. missouriana*	-	-	-	HQ288225	HQ288267
ALG111	*L. mitidjana*	-	-	-	MN104115	MN159114
CMW7060	*L. mutila*	-	-	-	AY236955	AY236904
CBS 456.78	*L. parva*	-	-	-	MH861166	EF622063
STE-U5803	*L. plurivora*	-	-	-	EF445362	EF445395
IBL12	*L. pontae*	-	-	-	KT151794	KT151791
CBS116459	*L. pseudotheobromae*	-	-	-	EF622077	EF622057
CBS121770	*L. pyriformis*	-	-	-	EU101307	EU101352
ZLNB6	*L. rubropurpurea*	-	-	-	OR534119	OR552384
CBS342.78	*L. sterculiae*	-	-	-	KX464140	KX464634
CMM3872	*L. subglobosa*	-	-	-	KF234558	KF226721
B0041	*L. thailandica*	-	-	-	KM006433	KM006464
CBS124.13	*L. theobromae*	-	-	-	DQ458890	DQ458875
CBS111530	*L. theobromae*	-	-	-	EF622067	EF622054
CPC175.26	*L. theobromae*	-	-	-	EF622067	EF622047

Table 2 (continued)

Isolate	Species*	Length of conidia (µm)	Width of conidia (µm)	Average L/W of conidia	GenBank Accession numbers	
					ITS	*tef1-α*
CBS118739	*L. venezuelensis*	-	-	-	KX464140	KX464634
UCD2553AR	*L. viticola*	-	-	-	HQ288227	HQ288269
LC12043	*Curvularia dactyloctenicola*	-	-	-	MN215652	MN263946
CPC28829	*C. chiangmaiensis*	-	-	-	MF490814	MF490857
LC12036	*C. chiangmaiensis*	-	-	-	MN215648	MN263942
LC12043	*C. dactyloctenicola*	-	-	-	MN215652	MN263946
LC11981	*C. lunata*	-	-	-	MN215676	MN263970
MFLUCC22-0142	*C. lunata*	-	-	-	OP802379	OP830873
CBS339.64	*C. pseudobrachyspora*	-	-	-	MN688816	MN688868
CBS533.70	*C. pseudobrachyspora*	-	-	-	MN688813	MN688866
BRIP15900	*C. sorghina*	-	-	-	KJ415558	KJ415435
CBS114979	Diaporthe arengae	-	-	-	KC343034	KC343760
MUS0028	D. drechsleri	-	-	-	KF500532	KM093761
CBS121124	D. corylina	-	-	-	KC343004	KC343730
CBS133811	*D. endophytica*	-	-	-	KC343065	KC343791
CBS444.82	*D. eugeniae*	-	-	-	KC343098	KC343824
ASHM304	*D. eugeniae*	-	-	-	MK110370	MK117250
CBS 129519	*D. musigena*	-	-	-	KC343143	KC343869
CBS809.85	*D. oncostoma*	-	-	-	KC343163	KC343889
CBS589.78	*D. oncostoma*	-	-	-	KC343162	KC343888
CBS101339	*D. pseudomangiferae*	-	-	-	KC343181	KC343907
CBS388.89	*D. pseudomangiferae*	-	-	-	KC343182	KC343908
CBS462.69	*D. pseudophoenicicola*	-	-	-	KC343184	KC343910
CBS176.77	*D. pseudophoenicicola*	-	-	-	KC343183	KC343909
LC8106	*D. yunnanensis*	-	-	-	KY491541	KY491551
CBS11851	*Fusarium ananatum*	-	-	-	KU604023	KU711690
CBS184.29	*F. ananatum*	-	-	-	KR071629	KU711689
CBS258.54	*F. annulatum*	-	-	-	MH857317	MT010994
CBS119858	*F.anthophilum*	-	-	-	KR071656	KU604428
CBS100057	*F. bactridioides*	-	-	-	MH862686	MN533993
CBS450.97	*F. concentricum*	-	-	-	MH862659	MT010992
LC7864	*F. fujikuroi*	-	-	-	MW016453	MW580493
CBS119853	*F. mangiferae*	-	-	-	MH863065	MN534016
CBS131377	*F. nygamai*	-	-	-	KU711707	KR071696
CBS140.95	*F.nygamai*	-	-	-	KR071695	KU711706
CBS140424	*F.oxysporum*	-	-	-	KT794176	KT794174
NFCCI 3282	*F.proliferatum*	-	-	-	ON003543	ON032438
CBS147.25	*F. sacchari*	-	-	-	MH854822	MW402099
CBS223.76	*F. sacchari*	-	-	-	KU604026	MW402115
ICMP18608	*Colletotrichum aenigma*	-	-	-	JX010244	NR_120140
ICMP17904	*C. boninense*	-	-	-	JX010292	GU174577
C07020	*C. coccodes*	-	-	-	GU935876	GU935836
C08021	*C. coccodes*	-	-	-	GU935878	GU935838
ACCC36361	*C. fructicola*	-	-	-	MF627898	MF627962

Table 2 (continued)

Isolate	Species*	Length of conidia (µm)	Width of conidia (µm)	Average L/W of conidia	GenBank Accession numbers	
					ITS	*tef1-α*
ICMP17974	*C. gloeosporioides*	-	-	-	GU174543	GU174568
ICMP17941	*C. gloeosporioides*	-	-	-	GU174547	GU174569
C08122	*C. higginsianum*	-	-	-	GU935873	GU935833
C97031	*C. higginsianum*	-	-	-	GU935871	GU935831
C1180.1	*C. horii*	-	-	-	GQ329690	JQ071901
C08048	*C. panacicola*	-	-	-	GU935867	GU935827
C08061	*C. panacicola*	-	-	-	GU935868	GU935828
FBR-42	*C. siamense*	-	-	-	MG867589	MH844549
LC0598	*C. tropicale*	-	-	-	KC790942	JQ071909
BRIP45094	*C. xanthorrhoeae*	-	-	-	JX010261	GU174575

*As determined by *tef1-α* sequence analysis

according to 5 fruits per isolate (with 3 replications). An agar plug without mycelium was applied on 5 fruits (with 3 repetitions) for control. The inoculated portion was wrapped with parafilm. Inoculated fruits were then incubated at 25 ± 2 °C with a relative humidity of 55 ± 2 % for 10 days. Fruits were checked daily for symptoms development. To satisfy Koch's postulate, pieces from diseased tissues of symptomatic fruits were removed, surface sterilized as mentioned above and plated on PDA. An isolate was considered pathogenic when it was able to cause disease symptoms (rot) and further isolated from the inoculated fruit. The morphological characteristics of the isolates were compared with those of the original isolates.

Statistical analysis

Mango SER incidence and severity data were checked for normal distribution and homogeneity, running Shapiro-Wilk and Levene tests, respectively. A series of analysis of variance (ANOVA) tests were performed to determine, successively, the effect of surveyed departments and locality on SER disease incidence and severity. In case of significant differences, means were separated using Tukey's test (P <0.05). Linear regression modele were subsequently conducted to evaluate the effect of weather parameters on SER incidence and severity. Furthermore, Correlation analysis was used to determine the association among variables, considering all climatic variables and mango SER incidence and severity. All analyses were performed using R software (R Core Team 2021).

Results

Incidence and severity of mango SER

SER incidence in orchards ranged from 10% to 30 %, while severity varied from 5% to 20 % (Table 1, Fig. 1A , B). Furthermore, the analysis revealed a strong positive correlation (r = 0.92) between the SER incidence and severity (Fig. 1E). The results reveal that the highest SER incidence were found in the localities of Odienné 2 (32%), Odienné 3 (20%) and Tchékpè (20%) (P<0.05). In addition, the localities of Odienné 2 and Tchépkè shown the highest SER severity with 24 and 18.4%, respectively (P<0.05) (Table 1). Regarding departments, the incidence of mango SER varied across different departments, with values of 11.3%, 12%, 14.7%, 19.3%, and 22% for the Boundiali, Sinématiali, Korhogo, Odienné, and Ferkéssédougou, respectively. Similarly, the severity followed a similar trend, with values of 7.6%, 9.4%, 11.8%, 19.8%, and 17.4%, in the same order for incidence. However, no significant differences were observed between departments for both variables (P > 0.05) (Table 1).

Effect of climate parameters on mango SER incidence and severity

The results of the correlation test between the average six-months climatic parameters prior to the survey and SER incidence and severity are presented in Fig. 2. The analysis revealed no correlation between PREC, RH2M, T2MDEW and T2M_MAX and the incidence and severity of SER as indicated by the null correlation coefficients (Fig. 2A, B). On the other hand, we observed a low positive

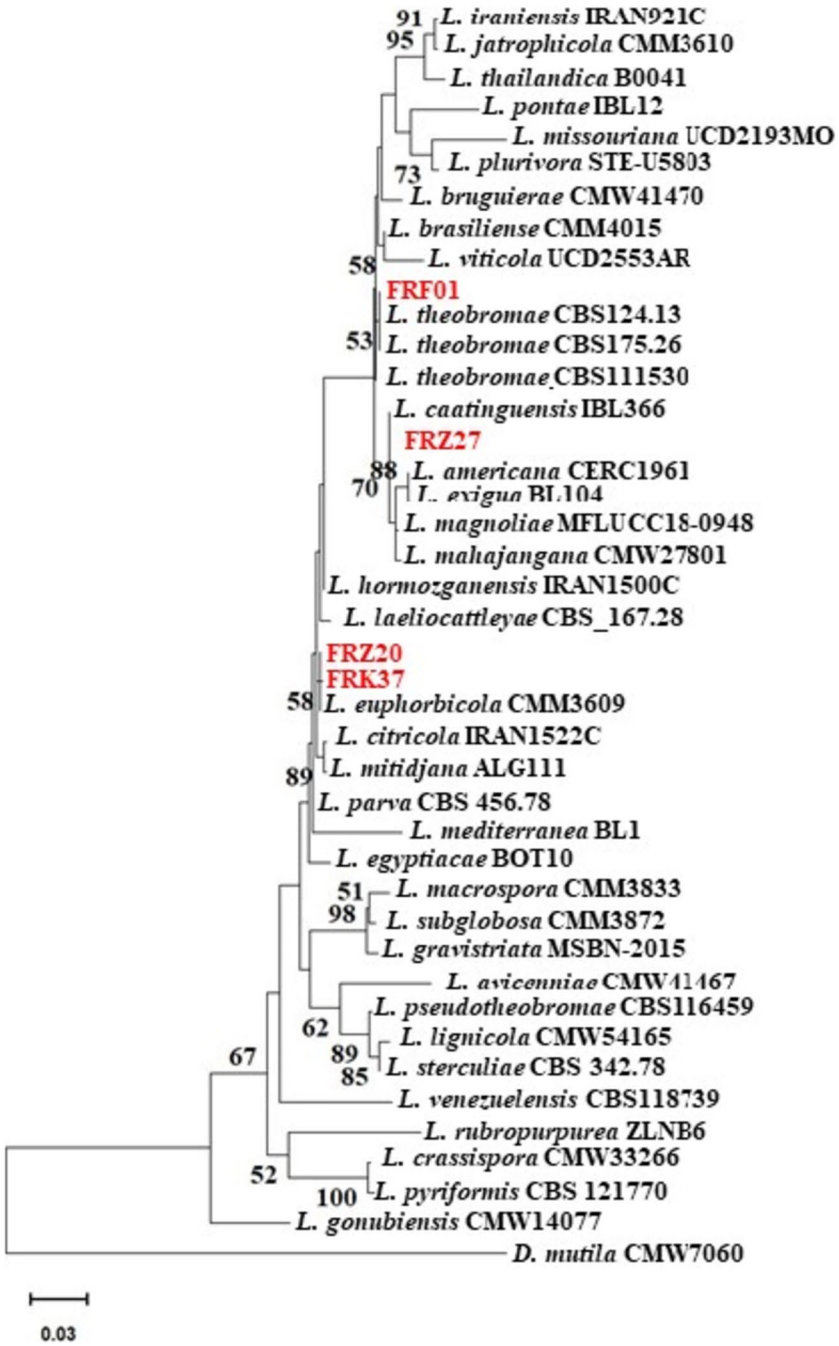

Fig. 4 Maximum likelihood tree of *Lasiodiplodia* species isolated from mango SER based on concatenated ITS and *tef1-α* genes sequences using Kimura 3-parameter model with 1000 bootstrap replications. The isolates from the current study are in red. The bootstrap support values above 50% are given at the node. This analysis involved 42 nucleotide sequences. There were a total of 825 positions in the final dataset. *Diplodia mutila* (CMW7060) is used as the outgroup taxon

correlation between T2M and T2M_MIN and the incidence of SER (Fig. 2A), with correlation coefficients of 0.36 and 0.26, respectively.

Fungi identification

Fungal colonies isolated from 350 fruits presenting SER symptoms were characterized by morphological characteristics of colonies growing on PDA or pine needles on WA. Five fungal genera were identified, including *Lasiodiplodia* sp. that were the most isolated (74 %), followed by *Colletotrichum* spp. (9 %), *Curvularia* spp. (7 %), *Diaporthe* spp. (6 %) and *Fusarium* spp. (4 %).

Lasiodiplodia spp. colonies on PDA reached 95 mm diameter in 7 days, produced dense aerial mycelium, initially white, then turned to dark brown and black (Figure 3a, b). Conidia were subovoid to ellipsoidovoid, with the apex broadly rounded, thick-walled, and contents granular; initially hyaline and aseptate, then dark brown and 1-septate with longitudinal striations (Fig. 3c). Conidia size was 13–30.9 µm length (avg. ±S.D = 21.8 ± 3.2 µm) × 9.0-17 µm width (avg. ±S.D = 13.0 ± 0.1 µm) (n = 50), (L/W ratio = 1.8).

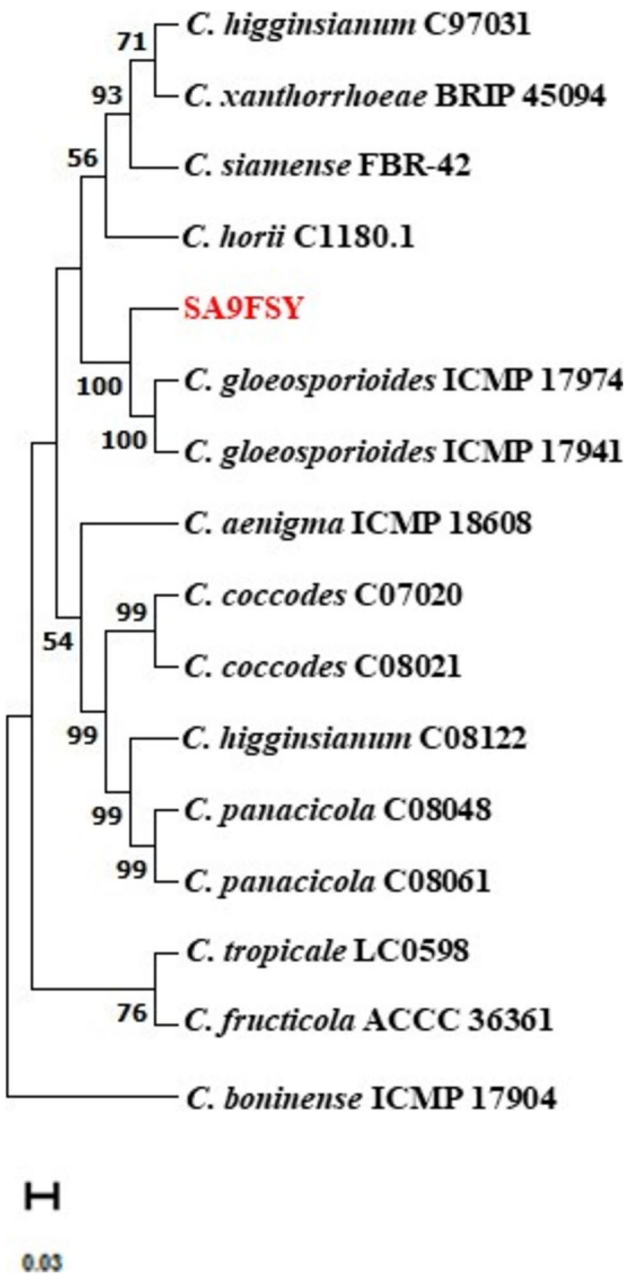

Fig. 5 Maximum likelihood tree of *Colletotrichum* species based concatenated ITS and *tef1-α* genes sequences using Tamura 3-parameter mode model with 1000 bootstrap replications. The species name and the strain from the current study are in red. The bootstrap support values above 50% are given at the nodes. This analysis involved 16 nucleotide sequences. There were a total of 503 positions in the final dataset. *Colletotrichum boninense* (ICMP 17904) is used as the outgroup taxon

Curvularia spp. fungal colonies on PDA reached 65–70 mm diameter in 7 days, exhibited gray, cotton-like mycelia with ring patterns on the plate (Fig. 8a). On the reverse plate, the pigmentation ranged from brown to blackish-brown (Fig. 8b). The conidia, either straight and ovoid or fusiform in shape, had two or three septa, with the middle septum being noticeably darker (Fig. 3c). Conidia were 15.8–25.2 µm length (avg. ±S.D = 20.4 ± 2.3 µm) × 9-12.0 µm width (av. ±S.D = 10.5 ± 1.5 µm) (n = 50), (L/W ratio = 1.9).

Fusarium spp fungal colonies reached 45–80 mm diameter in 7 days, displayed a white colouration (Fig. 3a, b). The micro and macroconidia were abundant, and their shape was hyaline, oval, or cylindrical (Fig. 3c). Macroconidia were 22.2-58.5 µm length (avg. ±S.D = 40.3 ± 3.2 µm) × 2-4.9 µm width (avg. ±S.D = 3.4 ± 1.1 µm) (n = 50), (L/W ratio = 11.7).

Colletotrichum spp. colonies on PDA reached 53–64 mm diameter in 7 days, displayed a pale olivaceous colouration, ranging from grey to olivaceous grey and merging into grey olivaceous at the centre (Fig. 3a). The reverse of the colonies appeared as iron grey to olivaceous black (Fig. 3b). Conidia were unicellular, hyaline, smooth or slightly roughened (Fig. 3c). Conidia were 14.8-20.5 µm length (avg. ±S.D = 17.6 ± 4.0 µm) × 5-6.2 µm width (avg. ±S.D = 5.6 ± 3.4 µm) (n = 50), (L/W ratio = 2.3).

Diaporthe spp. colonies reached 82–85 mm diameter in 7 days, mycelium had a white-grey appearance, with small clumps of scattered pycnidia (Fig. 3a). The ß conidia formed were unicellular, filiform, hyaline, aseptate smooth, spindle-shaped, and slightly curved (Fig. 8c). Conidia were 18.7-25 µm length (avg. ±S.D = 21.9 ± 7.0 µm) × 1-2 µm width (av. ±S.D = 1.5 ± 0.4 µm) (n = 50), (L/W ratio = 14.6).

Based on morphological characters and pathogenicity tests, four representative isolates of *Ladiodiplodia* spp. (Fr-F01; FRK37,FRZ20 and FRZ27) and one of *Colletotrichum* (SA9FSy), *Curvularia* (BenFFSy), *Fusarium* (1BRaA2) and *Diaporthe* (NTA) were selected for molecular identification (Table 2).

The isolates were then subjected to multigene DNA sequence analysis and identified at the species level (Table 1). BLASTn search of the consensus sequence (ITS and *tef1*-α) revealed 100 % identity with the reference sequences in GenBank for all isolates, which were identified as *Lasiodiplodia theobromae* (FRF01), *L. euphorbicola* (FRK37, FRZ20), *L. caatinguensis* (Fr-Z27), *Colletotrichum gloeosporioides* (SA9FSy), *Curvularia pseudobrachyspora* (BenFFSy), *Fusarium mangiferae* (1BRaA2) and *Diaporthe endophytica* (NTA). Furthemore, the phylogenetic analysis of the multigene DNA sequence based on ITS and *tef1*-α demonstrated that the SER sequences were similar to the reference sequences. Therefore, *Lasiodiplodia theobromae* (FRF01), *L euphorbicola* (FRK37, FRZ20), *L. caatinguensis* (Fr-Z27), *Colletotrichum gloeosporioides* (SA9FSy), *Curvularia pseudobrachyspora* (BenFFSy), *Fusarium mangiferae* (1BRaA2) and *Diaporthe endophytica* (NTA) showed a closed relationship to *Lasiodiplodia theobromae* (CBS 124.13 and CPC 27882), *L. euphorbicola* (CMM 3609), *L. caatinguensis* (IBL366), *Colletotrichum gloeosporioides* (ICMP 17974 and ICMP:17941), *Curvularia pseudobrachyspora* (CBS339.64 and CBS 533.70), *Fusarium mangiferae*

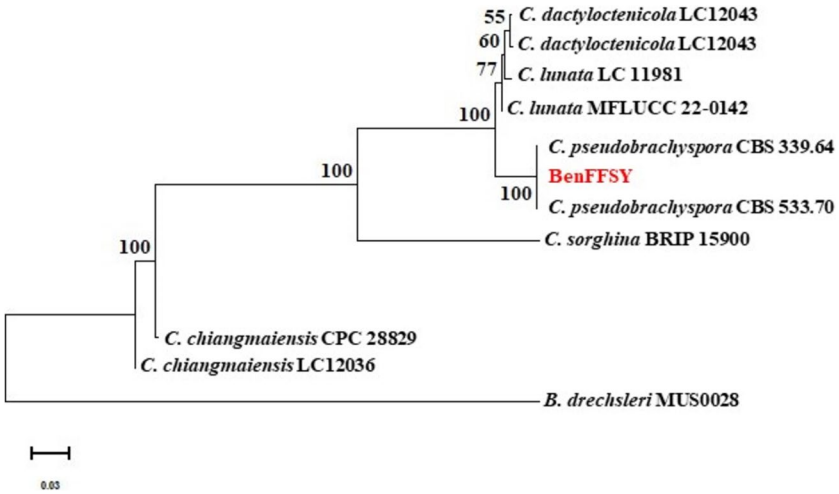

Fig. 6 Maximum likelihood tree of *Curvularia* species based on concatenated ITS and *tef1-α* genes sequences using Kimura 2-parameter model with 1000 bootstrap replications. The strain from the current study are in red. The bootstrap support values above 50% are given at the node. This analysis involved 13 nucleotide sequences. There were a total of 1374 positions in the final dataset. *Bipolaris drechsheri* (MUSOO28) is used as the outgroup taxon

(CBS 119853) and *Diaporthe endophytica* (CBS 133811), respectively (Fig. 4, 5, 6, 7 and 8). These analysis confirms the taxonomic classification and relationships between the studied isolates and their respective reference species.

Pathogenicity tests

The eight SER isolates inoculated on mango fruits induced peel discoloration during the incubation period. However, only *Lasiodiplodia theobromae* (FrF01), *L. euphorbicola* (FrK37, FrZ20), *L. caatinguensis* (FrZ27) and *Diaporthe endophytica* (NTA) isolates induced SER symptoms on the artificially inoculated fruits similar to those observed on naturally infected fruits. SER symptoms included a water-soaked, dark, discoloured area near the fruit stem, which could range from dark brown to purplish black (Fig. 9). These symptoms usually appeared on the ripe or ripening fruit peel at the stem-end region. At first, a dark-brown to black ring appeared around the pedicel, which expanded as the fruit ripened, covering the upper one-third of the fruit

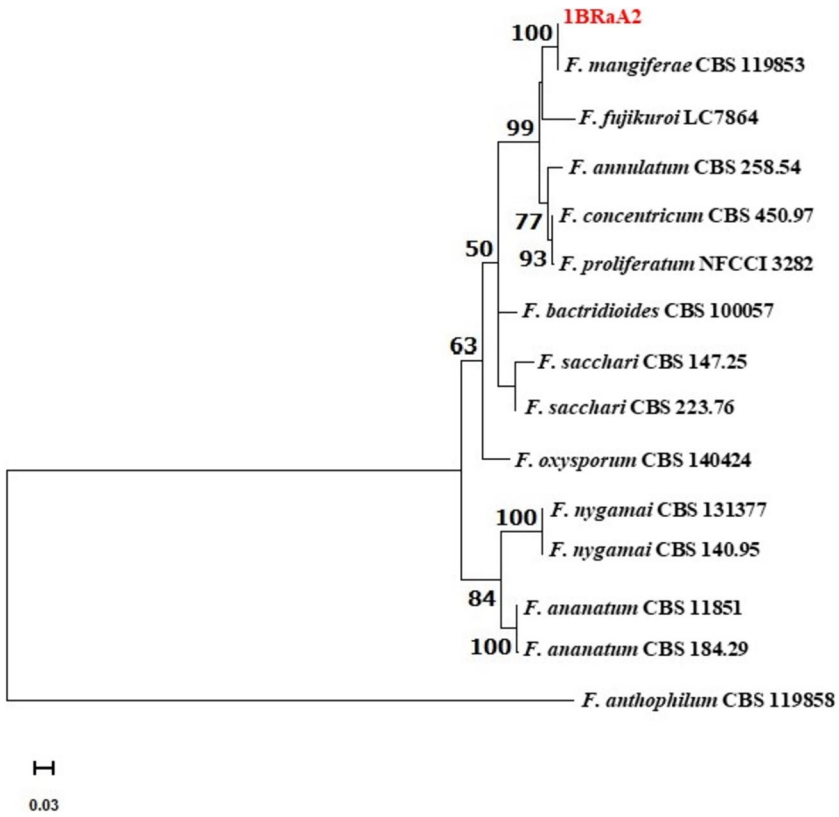

Fig. 7 Maximum likelihood tree of *Fusarium* species based on concatenated ITS and *tef1-α* genes sequences using Tamura-Nei model model with 1000 bootstrap replications. The species name, and the strain from the current study are in red. This analysis involved 15 nucleotide sequences. There were a total of 1091 positions in the final dataset. *Fusarium anthophilum* (CBS 119858) is used as the outgroup taxon

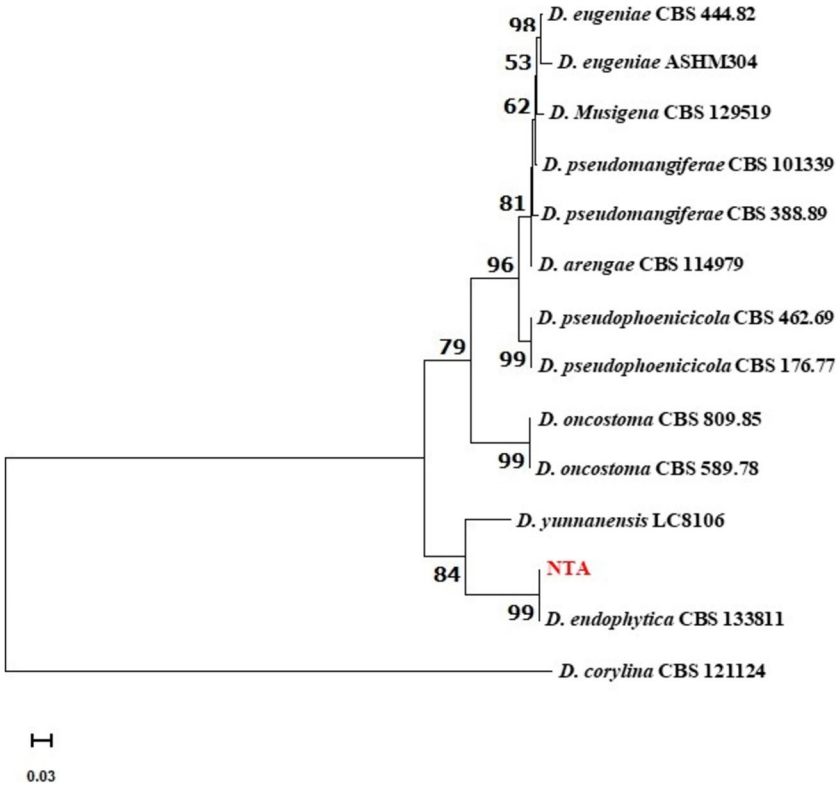

Fig. 8 Maximum likelihood tree of *Diaporthe* species based on concatenated ITS and *tef1-α* genes sequences using Hasegawa-Kishino-Yano model with 1000 bootstrap replications. The species name, and the strain from the current study are in red. The bootstrap support values above 50 % are given at the nodes. This analysis involved 14 nucleotide sequences. There were a total of 983 positions in the final dataset. *Diaporthe corylina* (CBS 121124) is used as the outgroup taxon

peel (Fig. 9a-e). As the infection progressed, the affected areas quickly darkened and merged, resulting in complete fruit rot 10 days after inoculation (DAI) (Fig. 9f). The fungi were reisolated on PDA, and the colony morphology and conidia produced in cultures were identical to the isolates of each species used originally for fruit inoculation.

Fruits showing SER symptoms had lesion dimensions ranging from 5 to 29 cm after 10 DAI. *Lasiodiplodia*

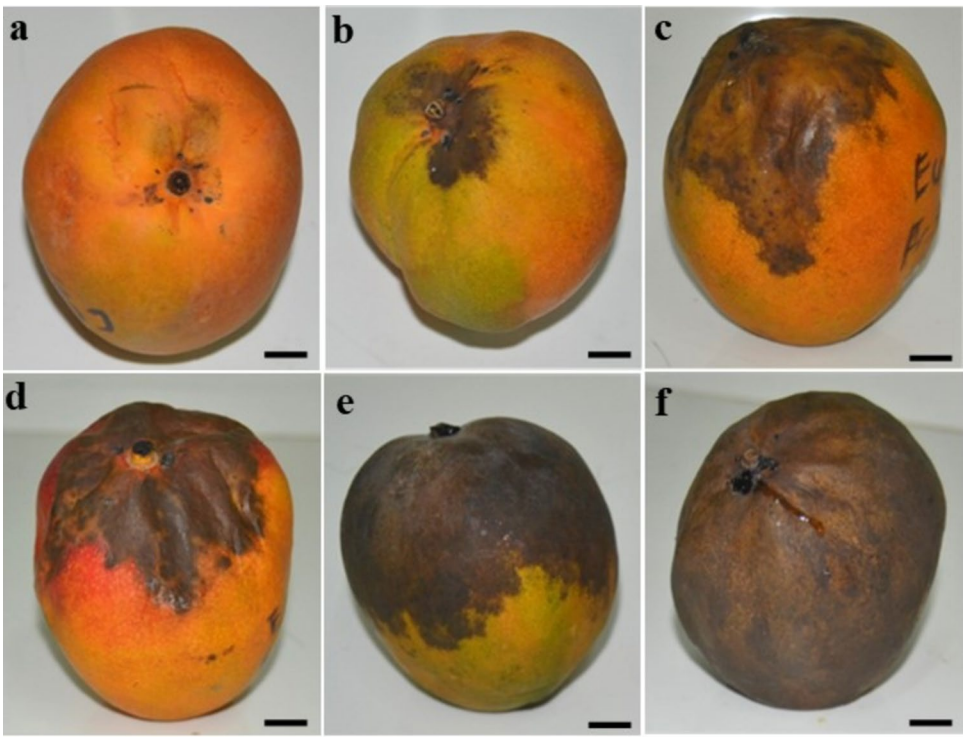

Fig. 9 Evolution of mango Stem-end rot (SER) symptoms on mango cv Kent fruits. **a=** First day of symptoms apparition: discoloration limited at the stem-end at 3 days after inoculation; **b=** 10% discoloration of the fruit surface area initiated by stem-end rot at 4 days after inoculation; **c=** 11-30% discoloration of the fruit surface area initiated by stem-end rot at 7 days after inoculation; **d=** 31-50% discoloration of the fruit surface area initiated by stem-end rot at 8 days after inoculation; **e=** more than 51% discoloration of the fruit surface area initiated by stem-end rot at 9 days after inoculation; **f=** fruit completely rotted (100 %) after 10 days after inoculation. Scales Bars = 2 cm

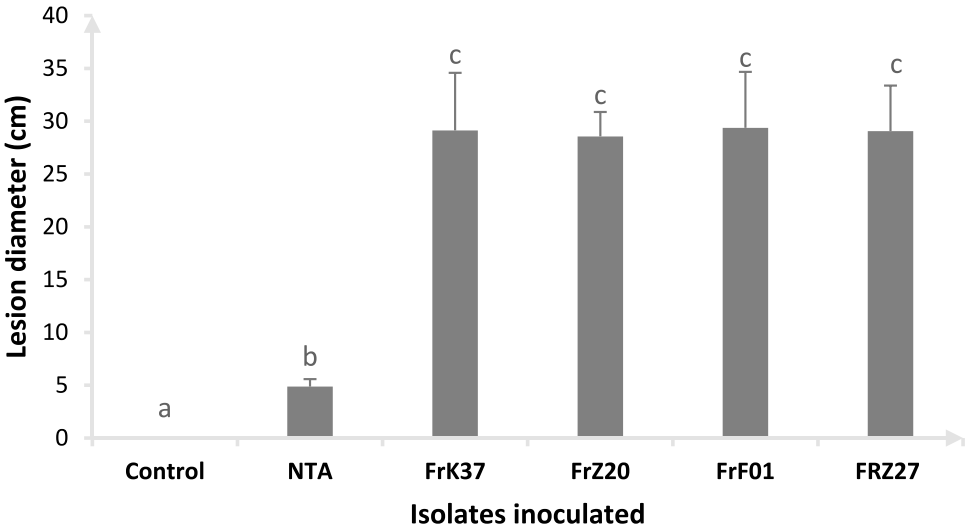

Fig. 10 Mango fruit lesion diameter at 10 days after inoculation with SER representatives isolates. NTA= *Diaporthe endophytica* FrK37, FrZ20 = *Lasiodiplodia euphorbicola*; FrF01= *L. theobromae*; FrZ27= *L. caatinguensis*. Values presented are mean ±SD (*n=15*). Values with different letters show a significant difference by ANOVA (p≤0.05), Tukey's range test at p=0.05

species were more virulent by inducing the largest lesion diameters: *Lasiodiplodia euphorbicola* FrK37 (29.12 cm), FrZ20 (28.56 cm), FRF01 (29.37 cm), and FRZ27 (29.06 cm). While *Diaporthe endophytica* (NTA) had the smallest lesion (5 cm) ($P < 0.05$) (Fig. 10). However, there was no statistically significant difference in diameter lesions amongst *Lasiodiplodia* isolates (Fig. 10).

Discussion

Mango SER poses a substantial challenge for all stakeholders in the mango industry, particularly farmers and export businesses. It is of utmost importance to undertake a comprehensive study of the epidemiology of SER disease in order to effectively manage and minimize the impact of this disease on mango production and quality. The current study evaluated mango SER intensity in the main production area in North West Côte d'Ivoire, determined the correlation between incidence and severity and preharvest climate parameters, and identified the SER causing fungi.

Symptoms of SER were characterized by the development of lesions that initially appeared as small, dark-brown to black areas located in the peel around the base of the fruit stem end. These lesions then progressed into a soft, watery rot that spread outwards from the peduncle, resulting in complete fruit rot after 10 days, as described by Galsurker et al. (2020) in Pakistan and Honger and William (2015) in Ghana.

Surveys conducted in 2020 and 2021 in different production departments indicated that SER is prevalent in the North West agroecological zone of the country. Depending on orchards, SER incidence varied between 10 to 30 % while severity was 5 to 20 %, with both variables having a strong positive correlation (Fig. 1). These results align with those found by Syed et al. (2017) in Pakistan and by Feygenberg et al. (2021) in Israel, who reported similar values. In addition, despite the SER incidence and severity varied between departments, no significant difference was found between them for both variables, suggesting that the geographical location may not significantly impact mango SER in this agroecological zone of Côte d'Ivoire. This result may be explained by the similarity of cultural practices and agroclimatic conditions prevailing in the selected orchards, as suggested by Syed et al. (2017) in Pakistan, where no statistically significant differences were observed in the incidence of postharvest rots among mango fruits collected from various regions of Sindh.

Storage temperature and relative humidity effect on mango SER incidence were reported by many authors worldwide (Alvindia and Acda 2015; Alam et al. 2017; Diskin et al. 2017). However, there is a limited data on the preharvest weather parameters effect on mango SER. The correlation analysis between climate parameters recorded during a six-months preharvest period and SER incidence and severity in orchards revealed a low positive correlation between the mean temperature (T2M) and the minimum temperature (T2M_MIN) with SER incidence ($r = 0.36$ and $r = 0.26$, respectively). These findings are consistent with previous research, notably those conducted by Riquelme-Toledo et al. (2020), Luck et al. (2011), Newton et al. (2011), and Colhoun (1973), indicating that environmental conditions are relevant variables affecting pathogen infection. Moreover, Honger and William (2015) identified that the district in Ghana with consistently high temperatures throughout

the year had the highest mango SER. However, the low correlation between mango SER incidence and severity with precipitation and relative humidity observed in our study may suggest that other factors, such as farmers' cultural practices and soil type, could also explain the intensity of the disease in these regions of Côte d'Ivoire (Wright and Grant, 1997; Ramírez-Gil et al. 2021).

The present study identified several fungal genera associated to mango SER, including *Lasiodiplodia*, *Curvularia*, *Fusarium*, *Colletotrichum* and *Diaporthe*. Among them, isolates belonging to the *Lasiodiplodia* genus were the most frequently isolated, with a 74% isolation rate. Assignment to species based on multigene phylogenetic analysis of ITS and *tef1-α* sequences may be chalenging for those genera where cryptic species have been recently denominated (Alves et al. 2008; Dissanayake et al. 2016). The species concept for filamentous fungi is still largely discussed and debated (Stengel et al. 2022). In this study, sequences obtained for SER isolates were identical to sequences deposited in GenBank for type isolates from seven species (with 100 % of percentage similarity for all isolates), namely *L. theobromae, L. caatinguensis*, *L. euphorbicola, C. gloeosporioides*, *F. mangiferae*, *C. pseudobrachyspora* and *D. endophytica*.

All Mango Stem-end Rot (SER) isolates were pathogenic towards fruit. Nonetheless, authentic SER symptoms were exclusively discerned in *Lasiodiplodia* species and *Diaporthe endophytica* isolates, with *Lasiodiplodia* species displaying the most aggressiveness. The dominance of *Lasiodiplodia* species hints at a potentially heightened propensity for inflorescence colonization in mangoes, which might account for the observed elevation in isolation rates. Our findings corroborate those of Karunanayake and Adikaram (2020), underscoring the preeminent role of *Lasiodiplodia* species as major pathogens responsible for SER in mango, particularly in arid and warmer regions across the globe.

As in the present study, the fungal genera *Colletotrichum*, *Curvularia*, *Diaporthe*, and *Fusarium* were reported to be associated with mango SER in several previous studies (Honger and William 2015; Guarnaccia 2016; Alam et al. 2017; Ajitomi et al. 2020). However, *C. gloeosporioides* is mainly known as the causal agent of mango anthracnose, which is characterized by small, circular, sunken spots that appear on the mango fruit surface (N'Guettia et al. 2013; Dembélé et al. 2020). Nevertheless, the symptoms are completely different from those of SER and should not be confused with it (Honger and William 2015). Recently, Adikaram et al. (2022) discovered *Curvularia* species causing stem-end browning symptoms (SEB) in mango, which are distinct from SER symptoms. About *Diaporthe* sp (syn *Phomopsis*), the main species reported on mango SER were *D. eugeniae*, *D. pascoei*, *D. perseae*, and *D. ueckerae* (Lim et al. 2019; Ajitomi et al. 2020). Our isolate was similar to *D. endophytica*, which has been isolated on SEB in ripe mango by Adikaram et al. (2022). Furthemore, we identified *F. mangiferae* on SER symptoms. It has also been previously reported on mango malformation in Sri Lanka (Kausar et al. 2021) and SEB disease in ripe mango (Adikaram et al. 2022). The presence of all these isolates concurrently isolated on SER symptoms could be explained by the fact that SER symptoms expanded and masked the lesions of the other fungal, as mentioned in the study conducted by Honger and William (2015).

Mango SER is one of the most important postharvest disease in mango production areas worldwide. This work showed that mango SER is prevalent in Côte d'Ivoire, with an incidence rate of up to 30 %. In addition, meteorological factors such as preharvest temperature are among the parameters that can influence this disease. Therefore, environmental factors could be included in the panel of control methods for SER. Furthermore, seven species of fungal pathogens were identified, with Botryosphaeriaceae (*Lasiodiplodia* spp) the most isolated family. By filling the knowledge gap on the epidemiology of the SER disease of mango in Côte d'Ivoire, our results establish a solid basis to guide future research on mango postharvest diseases. Therefore, a broader study and evaluation of mango plantations should be undertaken in future studies to better understand the relationship between overall mango infection and postharvest development of SER.

Acknowledgements The first author acknowledges the support from the Société Internationale d' Importation (SIIM, France) and the Société de Diverses Prestations et d'Exportations (Sodipex SARL, Côte d'Ivoire) for their technical support. We also thank mango producers for the facilities they provided us during the survey.

Author contributions Y.S.Y: Conceptualization; Methodology; Resources; Formal analysis ;Roles/Writing - original draft

D. K: Conceptualization; Funding acquisition . Project administration

Y. K: Methodology

D.D. D: Review & editing

E.L.D.G.A.: Roles/Writing - review & editing

JY.R: Funding acquisition; Writing - review & editing

E.M. D. P : Methodology; Formal analysis; Roles/Writing - review & editing

D.F: Conceptualization; Funding acquisition; Methodology; Formal analysis; Roles/Writing - review & editing

Funding This research was funded by the Partnership for Skills in Applied Sciences, Engineering, and Technology—Regional Scholarship and Innovation Fund (PASET-RSIF), the French Research Institute for Development (IRD, France), and the Fondation Louis Omer DECUGIS (OMER-DECUGIS & CIE - 94538 RUNGIS, FRANCE).

Data availability The datasets generated during and/or analysed during the current study are available from the corresponding author on reasonable request. Sequence data from this article can be found in the GenBank data libraries under the different accession numbers mentioned for ITS and *tef1- α* genes listed in Table 2.

Declarations

Conflict of interest E.M.D.P. is the editor-in-chief and D.F. is an associate editor for this journal and their manuscript was independently handled by another member of the editorial board

References

Adikaram NKB, Maharachchikumbura SSN, Yakandawala DMD, Manawadu LN, Dissanayake DMS, Jayasinghe L (2022) Postharvest stem-end browning (SEB) disease in ripe mango (*Mangifera indica* L.) cultivar TomEJC. Eur J Plant Pathol 165:447–464

Ajitomi A, Minoshima A, Takushi T, Truong HH, Ooshiro A, Yamashiro M, Arasaki C, Hirooka Y (2020) First report of mango (*Mangifera indica*) stem-end rot caused by two Diaporthe species and their susceptibility to procymidone. J Gen Plant Pathol 86:237–244. https://doi.org/10.1007/s10327-020-00921-7

Alam MW, Rehman A, Sahi ST, Malik AU (2017) Exploitation of natural products as an alternative strategy to control stem end rot disease of mango fruit in Pakistan. Pakist J Agric Sci 54:775–783

Alkan N, Kumar P (2018) Postharvest storage management of mango fruit. In: Galán Saúco V, Lu P (eds) Achieving sustainable cultivation of mango, pp 377–402

Alves A, Crous PW, Correia A, Phillips AJL (2008) Morphological and molecular data reveal cryptic speciation in *Lasiodiplodia theobromae*. Fungal Divers 28:1–13

Alvindia DG, Acda MA (2015) Revisiting the efficacy of hot water treatment in managing anthracnose and stem-end rot diseases of mango cv. "Carabao. Crop Protect 67:96–101

Colhoun J (1973) Effects of environmental factors on plant disease. Ann Rev Phytopathol 11:343–364

Dembele DD, Kamara A, Grechi I, Silué N, N'goran NS, Yéo YS, Rey JY, Koné D, (2020) Morphological characteristics and distribution of colletotrichum isolates morphotypes infecting mango (*Mangifera indica* L.) in the north of Côte d'Ivoire. Afr J Food, Agric Nutr Dev 20:15837–15856

Diedhiou PM, Mbaye N, Drame A, Samb PI (2007) Alteration of post harvest diseases of mango Mangifera indica through production practices and climatic factors. Afr J Biotechnol 6:1087–1094

Diskin S, Feygenberg O, Maurer D, Droby S, Prusky D, Alkan N (2017) Microbiome alterations are correlated with occurrence of postharvest stem-end rot in mango fruit. Phytobiomes J 1:117–127

Dissanayake AJ, Phillips AJL, Li XH, Hyde KD (2016) Botryosphaeriaceae : current status of genera and species. Mycosphere 7:1001–1073

FAO Statistics, Food and Agriculture Organization of the United Nations, Rome, Italy, 2021.https://www.fao.org/faostat/en/#home. Accessed on September 05, 2023

Feygenberg O, Diskin S, Maurer D, Alkan N (2021) Effect of biological and chemical treatments during flowering on stem-end rot disease, and mango yield. Plant Dis 105:1602–1609

Galsurker O, Diskin S, Duanis-Assaf D, Doron-Faigenboim A, Maurer D, Feygenberg O, Alkan N (2020) Harvesting mango fruit with a short stem-end altered endophytic microbiome and reduce stem-end rot. Microorganisms 8

Galsurker O, Diskin S, Maurer D, Feygenberg O, Alkan N (2018) Fruit stem-end rot. Horticulturae 4:1–16

Govender V, Korsten L, Sivakumar D (2005) Semi-commercial evaluation of bacillus licheniformis to control mango postharvest diseases in South Africa. Postharvest Biol Technol 38:57–65

Groppe K, Boller T (1997) PCR assay based on a microsatellite-containing locus for detection and quantification of Epichloë endophytes in grass tissue. Appl Environ Microbiol 63:1543–1550

Guarnaccia V, Vitale A, Cirvilleri G, Aiello D, Susca A, Epifani F, Polizzi G (2016) Characterisation and pathogenicity of fungal species associated with branch cankers and stem-end rot of avocado in Italy. Eur J Plant Pathol 146:963–976

Hall TA (1999) BioEdit: a user-friendly biological sequence alignment editor and analysis program for windows 95/98/NT. Nucleic Acids Symp Ser 41:95–98

Honger JO, William CE (2015) Pathogenicity and fungicide sensitivity of the causal agent of postharvest stem end rot disease of mango in Ghana. Ghana J Agric Sci 49:37–52

Johnson GI (2008) Statut of mango postharvest diseases management R&D: Horticulture Australia final report for project MG08017*:* 1-130.

Johnson GI, Mead AJ, Cooke AW, Dean JR (1992) Mango stem end rot pathogens - fruit infection by endophytic colonisation of the inflorescence and pedicel. Annalsof Appl Biol 120:225–234

Karunanayake KOLC, Adikaram NKB (2020) Stem-end rot in major tropical and sub-tropical fruit species. Ceylon J Sci 49:327–336

Kausar R, Iram S, Ahmad KS, Jaffri SB (2021) Molecular characterization of *Fusarium solani* and *Fusarium oxysporum* phyto-pathogens causing mango maturity malconformation. Arch Phytopathol Plant Protect 54:1372–1390

Kouamé GK, Sorho F, Koné D, Bomisso LE, Aké S, Yatty J (2011) Activité pathologique comparée de deux isolats de *Colletotrichum gloeosporioïdes* (PENZ.) sur deux varietés de mangues (*Mangifera indica* L.). Agronomie Africaine 23:33–41

Kouassi AO (2012) Revue Nationale pour identifier les initiatives de valorisation non alimentaire de la mangue en Côte d'Ivoire. Revue Nationale no12/Coleacp Paepard-01/BNA-12, p 43

Lim L, Mohd MH, Zakaria L (2019) Identification and pathogenicity of Diaporthe species associated with stem-end rot of mango (*Mangifera indica* L.). Eur J Plant Pathol 155:687–696

Luck J, Spackman M, Freeman A, TreBicki P, Griffiths W, Finlay K, Chakraborty S (2011) Climate change and diseases of food crops. Plant Pathol 60:113–121

Marques MW, Lima NB, De Morais MA, Barbosa MAG, Souza BO, Michereff SJ, Phillips AJL, Câmara MPS (2013) Species of Lasiodiplodia associated with mango in Brazil. Fungal Divers 61:181–193

N'Guettia MYN, Kouassi N, Diallo HA, Kouakou FRYY (2014) Evaluation of anthracnose disease of mango (*Mangifera indica* L.) fruits and characterization of causal agent in Côte d'Ivoire. Int J Agric Innov Res 2:1008–1017

N'Guettia YM, Diallo AH, Kouassi N, Coulibaly F (2013) Diversité morphologique et pathogénique des souches de Colletotrichum sp. responsables de l'anthracnose de la mangue en Côte d'Ivoire. J Anim Plant Sci 18:2775–2784

Newton AC, Johnson SN, Gregory PJ (2011) Implications of climate change for diseases, crop yields and food security. Euphytica 179:3–18

Owino WO, Ambuko JL (2021) Mango fruit processing: options for small-scale processors in developing countries. Agriculture 11:1105

Phillips AJL, Alves A, Abdollahzadeh J, Slippers B, Wingfield MJ, Groenewald JZ, Crous PW (2013) The Botryosphaeriaceae: genera and species known from culture. Stud Mycol 76:51–167

Pugnet V (2018) La mangue en Côte d'Ivoire. Fiche pays producteur. FruiTrop 255:78–84

R Core Team (2021) R: a language and environment for statistical computing. R Foundation for Statistical Computing. https://www.R-project.org/

Ramírez-Gil JG, Henao-Rojas JC, Morales-Osorio JG (2021) Postharvest diseases and disorders in avocado cv. Hass and their relationship to preharvest management practices. Heliyon 7:e05905. https://doi.org/10.1016/j.heliyon.2021.e05905

Riquelme-Toledo D, Valdés-Gómez H, Fermaud M, Zoffoli JP (2020) Postharvest incidence of stem end rot in 'Hayward' kiwifruit is related to preharvest Botrytis cinerea colonization of floral parts and latent infection. Plant Dis 104:823–832

Sparks A (2018) Nasapower: a NASA POWER global meteorology, surface solar energy and climatology data client for R. J Open Sour Softw 3:1035

Stengel A, Stanke KM, Quattrone AC, Herr JR (2022) Improving taxonomic delimitation of fungal species in the age of genomics and phenomics. Front Microbiol 13

Syed RN, Lodhi AM, Rajput NA, Kumbhar MI, Khanzada MA (2017) Prevalence of postharvest rots of mango in different farms of Sindh, Pakistan. Pakist J Botan 49:325–330

Tamura K, Stecher G, Kumar S (2021) MEGA 11: molecular evolutionary genetics analysis version 11. Mol Biol Evol 38:3022–3027

Terao D, Nechet KDL, Frighetto RTS, Anjos VDDA, Benato EA, Halfeld-Vieira BDA (2018) Physical postharvest treatments in the control of stem-end rot of mango. J Phytopathol 166:581–589

White TJ, Bruns T, Lee SJWT, Taylor J (1990) Amplification and direct sequencing of fungal ribosomal RNA genes for phylogenetics. PCR Protocols: A Guide to Methods and Applications 18:315–322

Wright PJ, Grant DG (1997) Effects of cultural practices at harvest on onion bulb quality and incidence of rots in storage. New Zealand J Crop Horticult Sci 25:353–358

Publisher's Note Springer Nature remains neutral with regard to jurisdictional claims in published maps and institutional affiliations.

Springer Nature or its licensor (e.g. a society or other partner) holds exclusive rights to this article under a publishing agreement with the author(s) or other rightsholder(s); author self-archiving of the accepted manuscript version of this article is solely governed by the terms of such publishing agreement and applicable law.